Experimental Investigation of the Sedimentation of a Dilute Fiber Suspension

Benjamin Herzhaft and Élisabeth Guazzelli
Laboratoire de Physique et Mécanique des Milieux Hétérogènes, URA 857 au CNRS, ESPCI, 10 rue Vauquelin, 75231 Paris Cedex 05, France

Michael B. Mackaplow and Eric S. G. Shaqfeh
Department of Chemical Engineering, Stanford University, Stanford, California 94305-5025
(Received 5 February 1996)

We consider the sedimentation of high aspect ratio fibers in a Newtonian fluid under Stokes' flow conditions. Measurements of the mean sedimentation velocity, variance of the sedimentation velocity, and the orientation distribution are presented using a modification of the novel experimental technique described by Nicolai *et al.* [Phys. Fluids **7**, 12 (1995)]. We find a steady state where the fibers "clump" together and tend to align in the direction of gravity with occasional "flipping." [S0031-9007(96)00601-1]

PACS numbers: 47.55.Kf, 47.15.Gf, 47.15.Pn, 82.70.Kj

The sedimentation of rigid spherical particles has been extensively studied in recent years [1]. Results for the mean sedimentation velocities in suspensions of spherical particles are available through analytical theories [2], extensive computer simulations [3,4], and a wide variety of experiments [1]. In general, it is found that the sedimentation velocity is strongly hindered by particle interactions, particularly through the *fluid backflow* [2]. However, there is less known about the sedimentation of nonspherical particles. For example, there have been few experimental studies which examine the means by which hydrodynamic interactions affect the settling of nonspherical particles. Turney *et al.* [5] have examined the sedimentation of polymethyl methacrylate rods using NMR imaging. They presented the hindered settling function for a range of volume loadings, all within the semidilute regime of particle concentration [6], but their measurements were based on the propagation of a broadening interface at the top of the particulate suspension. A second study was presented by Anselmet [7] where both the interface propagation speed and single particle velocities in the bulk were measured. Hindered settling functions were determined, though, because of the small size of the settling vessel, the sedimentation velocities were almost certainly affected by the proximity of the bounding walls.

From the theoretical perspective in the existing literature, there is reason to believe that the sedimentation of nonspherical particles, and particularly slender fibers, is qualitatively different than the sedimentation of spheres. For example, the sedimentation velocity of any axisymmetric, nonspherical particle under Stokes' flow conditions is sensitive to the particle orientation. Moreover, the orientation distribution function (for non-Brownian particles) is indeterminate under Stokes' flow conditions in the absence of interparticle interactions [8–10]. Therefore, without measurements or a theory which includes multibody interactions, the orientation distribution remains unknown and unpredicted. Note that in both experimental studies discussed above, the orientation distribution was only measured in the *initial* state and not after it had evolved over time. In an attempt to predict the orientation distribution, Koch and Shaqfeh [11] considered the sedimentation of axisymmetric, nonspherical particles in dilute suspension including only two-body interparticle interactions. Koch and Shaqfeh [11] demonstrated that due to the coupling between center-of-mass and orientational motion, particle "clumping" or "streaming" should occur. However, no mean sedimentation speeds or orientation distributions have been predicted from a rigorous theory.

It is the purpose of the present communication to report on experimental results which show that the sedimentation of nonspherical bodies can be qualitatively different than the sedimentation of spheres, precisely because of the coupling of the orientation distribution and the center-of-mass velocities. We show that, at least for a dilute suspension of slender fibers, this coupling produces a very inhomogeneous sedimenting suspension—one in which the inhomogeneities cause the sedimentation speed to *increase* over the maximum possible sedimentation speed of isolated particles. The implication is that the sedimentation of spherical particles is a singular limit, and that, for any particles characterized by a microstructural variable (such as orientation) which couples to the sedimentation velocity, there is no reason to suppose that either the suspension is homogeneous or the sedimentation is "hindered" by particle interactions.

Toward the goals described above, we have developed an experimental system to measure the mean sedimentation velocity and orientation distribution in the bulk of an evolving suspension of well-characterized nonspherical, axisymmetric particles. Our system is an enhanced and modified version of the experimental apparatus used by Nicolai *et al.* [12] in their investigation of spherical particles. Experiments were performed in a glass walled cell of rectangular cross section with an inside width of 10.00 ± 0.05 cm, an inside depth

 0031-9007/96/77(2)/290(4)$10.00

of 8.00 ± 0.05 cm, and a height of 50.00 ± 0.05 cm. An index-of-refraction matched fiber suspension was introduced into this vessel. The particles were glass rods manufactured by Mo-Sci Corporation (Rolla, Missouri) with index of refraction 1.473 ± 0.001, density $\rho_p = 2.25 \pm 0.12$ g/cm^3, length $l_p = 0.108 \pm 0.025$ cm, and diameter $d_p = 0.0102 \pm 0.0007$ cm. The Newtonian fluid was an organic mixture of 15% Santicizer 97 and 85% Santicizer 431 (both produced by Monsanto). The matching of the refractive index of the fluid with that of the glass rods of the suspension was ensured by air-conditioning the laboratory room at 22 ± 1 °C . At this temperature, the fluid viscosity was $\eta_f = 5.5 \pm 0.5$ P, and the fluid density was $\rho_f = 1.07 \pm 0.01$ g/cm^3. A number of fibers were marked with a thin coating of silver so that they could be tracked as described below. The particle volume fraction of the suspension was kept constant at $(0.48 \pm 0.03)\%$ for all the experiments. The important effective particle volume fraction is $n(l_p/2)^3 = 0.09 \pm 0.03$, where n is the number of particles per unit volume. It is defined in terms of the interaction length of fibers which is their "long" length, since velocity disturbances do not decay until one is at a distance l_p from a given fiber. The suspension examined here was therefore truly dilute since $n(l_p/2)^3 < 1$. The fiber Reynolds number defined as $l_p V_{s\|} \rho_f / \eta_f$ was smaller than 10^{-3}, where $V_{s\|} = 0.006 \pm 0.001$ cm/s is the theoretical value of the Stokes' velocity of an isolated vertically oriented fiber, i.e., the maximum velocity that an isolated fiber can achieve. Finally, the Péclet number, $Pe = l_p V_{s\|}/2D_{\rm cm}$ (where $D_{\rm cm}$ is the center-of-mass diffusivity), was in excess of 10^9, and, therefore, thermal fluctuations were irrelevant to the development of the suspension.

The cell was uniformly lit from behind, and the marked fibers which were previously mixed with the unmarked fibers were then easily tracked with a real time digital imaging system. Each sedimentation experiment consisted of carefully mixing the suspension with a small propeller and then tracking a marked fiber along the vertical direction of the cell through about 10 imaging windows of 1 cm $\times$ 1 cm. The starting time of the tracking ($t = 0$) corresponded to the cessation of mixing. The marked fiber was tracked first in the upper window, and then, when it reached the window bottom, the imaging system was lowered and the particle was tracked in the next window which had a small overlap with the upper window, and so on. The imaging windows were located in the median vertical plane of the cell far from the sedimentation front, the sediment layer, and the cell walls. The depth of field of the imaging system was about 3 cm. For all experiments, the length of the marked fiber corresponded to approximately 50 pixels and its diameter to 5 pixels.

The imaging system consisted of a charged coupled device video camera (512×512 pixels) connected to a fast and intelligent image processing and acquisition board (Matrox Image 1280), located in a personal computer operating with a digital imaging software (VISILOG 4.1 by Noesis). The tracking was achieved in real time with a specially designed program which allowed the location of the projection of the center of mass and the measurement of the projection of the orientation of the marked fiber onto the imaging window plane. The horizontal and vertical coordinates, $X_\perp$ and $X_\|$, respectively, of the projected center of mass and the projected angle, ϕ, of the fiber orientation (measured from the horizontal direction) were recorded as a function of time, t, into a file. The experimental error in the measurement of the center of mass was of the order of 0.2 pixel and that in the measurement of the projected angle was 5×10^{-4} rad. The sampling time, that is, the time between two recordings, had an average value of 2 s. This sampling time was always smaller than the time a fiber takes to traverse the recording window (at least of the order of 100 s). Horizontal and vertical instantaneous velocities of the fiber were calculated over each sampling time. In order to provide a statistically satisfactory data ensemble, 22 fibers were tracked over a distance of approximately 10 cm. In addition to these long trajectories, the other marked fibers which were present in each imaging window were also recorded. This gave an additional number of 897 fibers tracked over a distance of approximately 1 cm.

The horizontal and vertical instantaneous velocities made dimensionless by $V_{s\|}$, $V_\perp^*$, and $V_\|^*$, and the instantaneous projected angle, ϕ, of a typical fiber are plotted as a function of time in Fig. 1. In the remainder of the paper, all the measured quantities have been made dimensionless with the length scale $l_p/2$ and the time scale $l_p/2V_{s\|}$. The dimensionless horizontal instantaneous velocity, $V_\perp^*$, fluctuates about zero while the dimensionless vertical

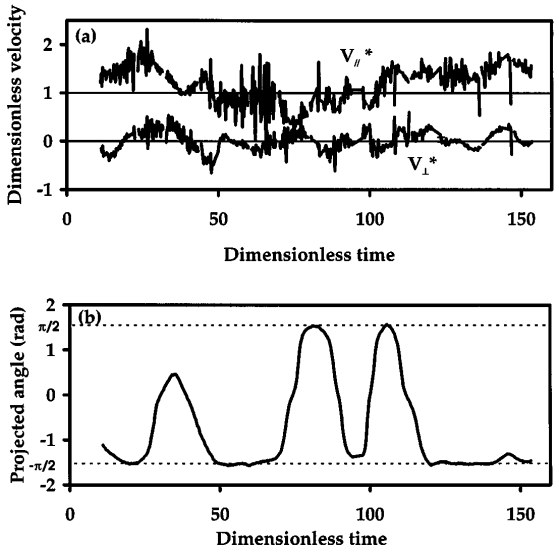

FIG. 1. (a) Instantaneous velocities, $V_\perp^*$ and $V_\|^*$, and (b) projected angle, ϕ, of a typical fiber versus time. The velocities are made dimensionless by scaling with $V_{s\|}$, and the time is made dimensionless by scaling with $l_p/2V_{s\|}$. The experimental uncertainty in $V_\perp^*$ is $\simeq 0.001$, that in $V_\|^*$ is $\simeq 0.3$, and that in ϕ is 5×10^{-4} rad.

instantaneous velocity, $V_{\|}^{*}$, reaches values in excess of unity. Both the horizontal and vertical velocities are characterized by large fluctuations. After a certain dimensionless time of approximately 50, the fiber aligns in the vertical direction with occasional "flipping" about this alignment. Note that tracked fibers with different starting heights present the same behavior.

In order to determine whether a steady state can be reached, the dimensionless mean velocities, $\langle V_{\perp}\rangle^{*}$ and $\langle V_{\|}\rangle^{*}$, and the mean projected angle, $\langle|\phi|\rangle$, ensemble averaged over all fiber trajectories are plotted versus dimensionless time, t^{*}, in Fig. 2. For each time, t, the number of instantaneous velocities (or projected angles) used in the statistical ensemble varied between 20 and 70. This number was found sufficient to reduce noticeably the statistical fluctuations. The dimensionless velocities seem to reach a steady state after a dimensionless time $t^{*} \simeq 50$, where $\langle V_{\perp}\rangle^{*}$ fluctuates around zero and $\langle V_{\|}\rangle^{*}$ around a value larger than 1. The mean projected angle $\langle|\phi|\rangle$ also reaches a steady state after the same time, where it fluctuates around a value of about 1.2 rad. Note that this value is smaller than the value of $\pi/2$ rad which corresponds to fibers perfectly aligned in the vertical direction. This is due to the fact that, at each time t, there is always a certain number of flipping fibers.

After steady state is reached ($t^{*} > 50$), we can assume the validity of the ergodic hypothesis. Histograms of all instantaneous velocities for different fiber trajectories can then be computed, and assumed to represent the statistics of many independent fiber trajectories [see Fig. 3(a)]. The number of data in each histogram is of the order of 2×10^{4}. The measured mean horizontal velocity is zero within error bars while the vertical velocity is $\langle V_{\|}\rangle^{*} = 1.5 \pm 0.3$, i.e, larger than the Stokes' velocity of an isolated vertical fiber. The dimensionless horizontal and vertical standard deviations are $\sigma_{v\perp}^{*} = 0.6 \pm 0.1$ and $\sigma_{v\|}^{*} = 1.3 \pm 0.2$, where the errors are the experimental errors. Thus, the vertical velocity fluctuations are found to be very large ($\simeq$100% of the mean). The ratio between the vertical and horizontal fluctuations, $\sigma_{v\|}/\sigma_{v\perp}$, which characterizes the anisotropy of the velocity fluctuations, is approximately 2. Note that the present relative vertical fluctuations and anisotropy are of the same order of magnitude as those found for the sedimentation of a suspension of spheres with a particle volume fraction of 10% [12]. We also mention that, while the histogram of the horizontal velocities seems approximately symmetric, that of the vertical velocities does not, as the latter has an asymmetric tail extending out towards positive values. The histogram of all projected angles for different fibers can be computed in the same manner after steady state has been achieved [see Fig. 3(b)]. Clearly, the probability for a fiber to align in the direction of gravity becomes very large. Note that a small local maximum in the histogram is observed around $\phi = 0$. Furthermore, we mention that two sets of fiber data were used to produce the results of Figs. 2 and 3. The first set corresponds to the 22 long trajectory fibers whose starting heights were located at the top of the bulk region of the suspension between the two fronts. The second set corresponds to the 897 marked fibers which were present in each imaging window and whose starting heights were thereby distributed along the cell. The statistics (mean and variance) coming from the two sets are identical. This finding suggests that the behavior is independent of the starting height.

In order to examine whether the suspension remains homogeneous during the sedimentation process, visualizations of the suspension structure were also undertaken. Experiments were performed in a smaller glass walled

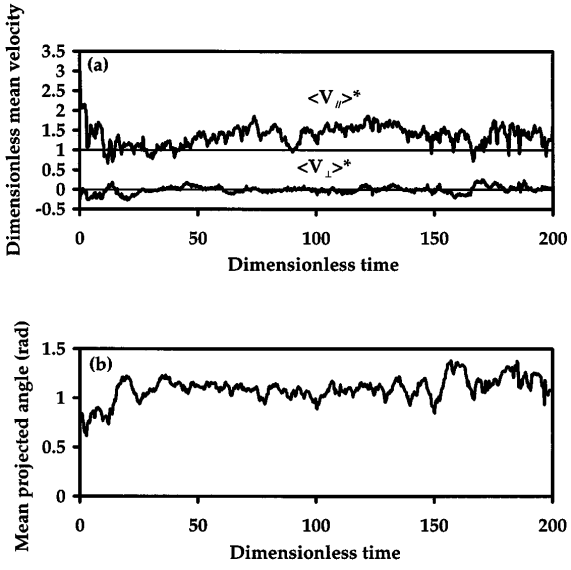

FIG. 2. (a) Mean velocities, $\langle V_{\perp}\rangle^{*}$ and $\langle V_{\|}\rangle^{*}$, and (b) mean projected angle, $\langle|\phi|\rangle$, versus time. The velocities are made dimensionless by scaling with $V_{s\|}$, and the time is made dimensionless by scaling with $l_p/2V_{s\|}$. The statistical uncertainty in $\langle V_{\perp}\rangle^{*}$ is $\simeq$0.004, that in $\langle V_{\|}\rangle^{*}$ is $\simeq$0.3, and that in $\langle|\phi|\rangle$ is $\simeq$0.1 rad. These statistical uncertainties represent the 68% confidence limit.

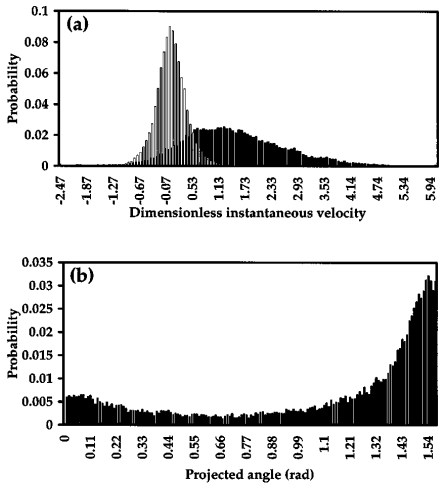

FIG. 3. Histograms (a) of the horizontal (open bars) and vertical (solid bars) instantaneous velocities, and (b) of the projected angles. The velocities are made dimensionless by scaling with $V_{s\|}$.

cell of rectangular cross section with an inside width of 6.50 ± 0.05 cm, an inside depth of 3.50 ± 0.05 cm, and a height of 40.00 ± 0.05 cm. The fluid, fibers, and particle volume fraction were the same as those of the previous experiment. However, all the fibers were silvered in this experiment. The structure of the suspension was easily observed when the cell was uniformly lit from behind. The experiment consisted of carefully mixing the suspension and then recording an imaging window of approximately 1 cm $\times$ 1 cm versus time (the starting time $t = 0$ corresponded again to the cessation of the mixing). The recorded window was located in the middle of the cell, far from the sedimentation front, the sediment layer, and the cell walls. The depth of field was chosen to be very small ($\simeq$0.5 cm) in order to record a vertical sheet of the suspension. Figure 4 presents 4 images of the suspension recorded at different times. Just after the initial mixing [see Fig. 4(a)], the suspension seems to be well stirred. At a later time [see Fig. 4(b)], the fibers start to "clump" and thus form slightly elongated packets. For $t^* > 50$ [see Figs. 4(c) and 4(d)], the "clumps" or "packets" appear to stop growing in size, and this is consistent with our observation that the mean vertical sedimentation velocity ceases to change with time. However, clearly more observations are necessary in order to determine whether a real steady state has been achieved. The observed size of the inhomogeneities or clumps appears to be approximately consistent with the wavelength of the most highly amplified instability mode as predicted by the linear stability analysis of Koch and Shaqfeh [11] ($\sim O([nl_p^3/8]^{-1/2} l_p) \sim 3 - 4$ fiber length in the present system). Note that there is clearly a *distribution* of clump sizes, and some are significantly larger than a few particle lengths in size.

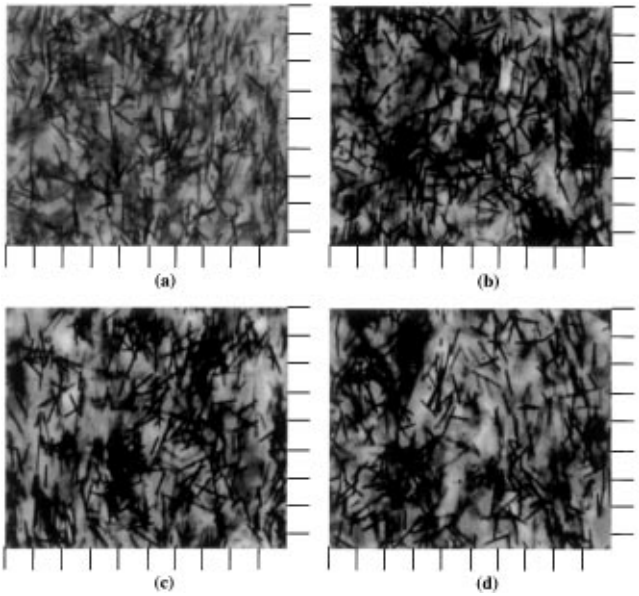

FIG. 4. Photos of the suspension structure: (a) $t^* = 11 \pm 2$, (b) $t^* = 21 \pm 4$, (c) $t^* = 78 \pm 14$, (d) $t^* = 129 \pm 24$. The horizontal (or vertical) scale is 1 mm.

To conclude, we have developed via modification of an existing experimental apparatus a very accurate technique for measuring the mean sedimentation velocity, its variance, and the orientation distribution of fibers in the bulk of a settling suspension. Our initial results at a value of $n(l_p/2)^3 = 0.09 \pm 0.03$ show that the suspension reaches a steady state where (i) the fibers tend to strongly align in the direction of gravity with occasional "flips," the latter of which create a slight broadening in the final ensemble-averaged distribution; (ii) the vertical mean sedimentation speed is not hindered and, in fact, is found to be larger than the Stokes' velocity of an isolated vertical fiber; and (iii) the velocity fluctuations are found to be very large and anisotropic. These findings, as well as visualizations of the suspension structure, suggest that the well-stirred suspension is unstable and that the fibers clump together to form slightly elongated packets which ultimately seem to stop growing in size. These packets settle faster than an isolated vertical fiber. The observed occasional flips of the fibers may be due to large shear stresses between the dense and light regions of the suspension. Further work is necessary to understand this fiber clumping mechanism, and to examine whether the well-stirred suspension is unstable at all particle volume fractions and aspect ratios.

The authors wish to thank E. J. Hinch for his helpful comments and suggestions during the development of this work. The work of B. H. is sponsored by the Ministère de l'Éducation Nationale, de l'Enseignement Supérieur et de la Recherche. This work and the collaboration was made possible via an NSF travel grant (No. INT-9016321) and a visiting professorship made available to E.S.G.S. through the ESPCI. We would also like to acknowledge additional support through the Merck Co. for a fellowship to M. B. M. The Santicizer 97 and Santicizer 431 were donated by Monsanto.

[1] R. H. Davies and A. Acrivos, Annu. Rev. Fluid Mech. **17**, 91 (1985).
[2] G. K. Batchelor, J. Fluid Mech. **52**, 245 (1972).
[3] J. F. Brady and G. Bossis, Annu. Rev. Fluid Mech. **20**, 111 (1988).
[4] A. J. C. Ladd, Phys. Fluids **5**, 299 (1993).
[5] M. A. Turney, M. K. Cheung, M. J. McCarthy, and R. L. Powell, AICHE J. **41**, 251 (1995).
[6] M. Doi and S. F. Edwards, *The Theory of Polymer Dynamics* (Clarendon Press, Oxford, 1986).
[7] M.-C. Anselmet, Thèse, Université de Provence, 1989 (unpublished).
[8] G. B. Jeffery, Proc. R. Soc. London A **102**, 161 (1923).
[9] J. Happel and H. Brenner, *Low Reynolds Number Hydrodynamics* (Prentice-Hall, Englewood Cliffs, NJ, 1965).
[10] L. G. Leal, Annu. Rev. Fluid Mech. **12**, 435 (1980).
[11] D. L. Koch and E. S. G. Shaqfeh, J. Fluid Mech. **209**, 521 (1989)
[12] H. Nicolai, B. Herzhaft, E. J. Hinch, L. Oger, and E. Guazzelli, Phys. Fluids **7**, 12 (1995).